



HAL
open science

Long-Range Order in the Dipolar XY Antiferromagnet $\text{Er}_2\text{Sn}_2\text{O}_7$

S. Petit, Elsa Lhotel, F. Damay, P. Boutrouille, A. Forget, D. Colson

► **To cite this version:**

S. Petit, Elsa Lhotel, F. Damay, P. Boutrouille, A. Forget, et al.. Long-Range Order in the Dipolar XY Antiferromagnet $\text{Er}_2\text{Sn}_2\text{O}_7$. *Physical Review Letters*, 2017, 119 (18), pp.187202. 10.1103/PhysRevLett.119.187202 . cea-01633911

HAL Id: cea-01633911

<https://cea.hal.science/cea-01633911>

Submitted on 13 Nov 2017

HAL is a multi-disciplinary open access archive for the deposit and dissemination of scientific research documents, whether they are published or not. The documents may come from teaching and research institutions in France or abroad, or from public or private research centers.

L'archive ouverte pluridisciplinaire **HAL**, est destinée au dépôt et à la diffusion de documents scientifiques de niveau recherche, publiés ou non, émanant des établissements d'enseignement et de recherche français ou étrangers, des laboratoires publics ou privés.

Long range order in the dipolar XY antiferromagnet $\text{Er}_2\text{Sn}_2\text{O}_7$

S. Petit,^{1,*} E. Lhotel,^{2,†} F. Damay,¹ P. Boutrouille,¹ A. Forget,³ and D. Colson³

¹Laboratoire Léon Brillouin, CEA, CNRS, Université Paris-Saclay, CE-Saclay, 91191 Gif-sur-Yvette, France

²Institut Néel, CNRS and Université Grenoble Alpes, 38042 Grenoble, France

³Service de Physique de l'Etat condensé, CEA, CNRS, Université Paris-Saclay, CE-Saclay, 91191 Gif-sur-Yvette, France

$\text{Er}_2\text{Sn}_2\text{O}_7$ remains a puzzling case among the extensively studied frustrated compounds of the rare-earth pyrochlore family. Indeed, while a long-range ordering towards an antiferromagnetic state with the so-called Palmer-Chalker structure is theoretically predicted, it has not been observed yet, leaving the issue, as to whether it is a spin-liquid candidate, open. In this letter, we report on neutron scattering and magnetization measurements which evidence the transition towards this Palmer-Chalker ordered state around 108 mK. Extreme care was taken to ensure a proper thermalization of the sample, which has proved to be experimentally crucial to successfully observe the magnetic Bragg peaks. The exchange parameters, refined from a spin wave analysis in applied magnetic field, confirm that $\text{Er}_2\text{Sn}_2\text{O}_7$ is a realization of the dipolar XY pyrochlore antiferromagnet. The inelastic spectra show at $T \lesssim T_N$ new features stemming from the Palmer-Chalker Bragg peaks and superimposed on a strong quasielastic signal. The proximity of competing phases and the strong XY anisotropy of the Er^{3+} magnetic moment might be at the origin of enhanced fluctuations and unconventional excitations.

Frustration in magnetism is usually characterized by the inability of a system to condense into an ordered state, even well below the temperature range of the magnetic interactions [1]. This reflects the presence, at the classical level, of a large ground state degeneracy, which prevents the system from choosing a unique ground state. Nevertheless, the system may eventually order owing to the presence of additional terms in the Hamiltonian, like second neighbor or Dzyaloshinski-Moriya interactions, or owing to “order by disorder” phenomena [2, 3], which lift the degeneracy and stabilize a unique ordered state. Conversely, fluctuations, originating for example from the proximity of competing phases, can hinder magnetic ordering, resulting in an unconventional correlated state with exotic excitations.

The pyrochlore oxide $\text{Er}_2\text{Sn}_2\text{O}_7$ appears to belong to this category. In this compound, the Er^{3+} magnetic moments reside on the vertices of a lattice made of corner sharing tetrahedra, and are confined by a strong XY anisotropy within local planes, perpendicular to the $\langle 111 \rangle$ axes. The magnetic interactions are found to be governed by dipolar interactions, in addition to a quasi-isotropic antiferromagnetic exchange tensor [4]. Mean field calculations show that, in the $T = 0$ phase diagram, this interaction tensor locates $\text{Er}_2\text{Sn}_2\text{O}_7$ in an antiferromagnetic phase, called “Palmer-Chalker” phase [5] (see Figure 1), close to the boundary with another ordered phase, the so-called ψ_2 phase which is realized in the related compound $\text{Er}_2\text{Ti}_2\text{O}_7$ [6]. The predicted Néel temperature is about $T_N^{\text{MF}} \approx 1.3$ K. Monte-Carlo simulations [7] have pointed out that fluctuations tend to lower the ordering temperature, reaching a lower critical temperature $T_N^{\text{MC}} \approx 200$ mK.

Experimentally, no phase transition has been detected down to about 100 mK in $\text{Er}_2\text{Sn}_2\text{O}_7$ up to now, yet Palmer-Chalker like short-range correlations have been



FIG. 1. (Color online) Sketch of the three configurations corresponding to the Palmer-Chalker ground state. The local XY planes perpendicular to the $\langle 111 \rangle$ axes are indicated by colored disks. In the Palmer-Chalker configurations, spins are pairwise anti-parallel, and collinear with an edge of the tetrahedron. These configurations can be described as chiral spin crosses.

reported below 5 K, taking the form of a broad diffuse quasielastic signal in neutron scattering measurements [4, 8]. In this letter, using neutron diffraction and magnetization measurements, we show that $\text{Er}_2\text{Sn}_2\text{O}_7$ does order, as expected, in the Palmer-Chalker state at a Néel temperature $T_N \approx 108$ mK. This long range ordering is characterized by magnetic Bragg peaks which develop on top of the broad diffuse scattering. The latter disappears progressively as the ordered magnetic moment increases. Concomitantly, the slow dynamics previously observed in ac susceptibility above the magnetic transition persists at low temperature and coexists with the Palmer-Chalker ordering. In addition, on entering the ordered phase, inelastic neutron scattering (INS) experiments reveal new features in the spin excitation spectrum stemming from the magnetic Bragg peaks on top of the quasielastic signal. Using INS measurements performed in applied magnetic field, we determine the exchange parameters of a model Hamiltonian, confirming previous

estimations.

Magnetization and ac susceptibility measurements were performed on a SQUID magnetometer equipped with a dilution refrigerator developed at the Institut Néel [9]. Neutron diffraction experiments were performed on the G4.1 cold neutron diffractometer (LLB-Orphée facility) with a wavelength $\lambda = 2.426$ Å. INS measurements were carried out on the triple axis spectrometer 4F2 using a final wavevector $k_f = 1.15$ Å⁻¹. The sample was a pure polycrystalline Er₂Sn₂O₇ compound, synthesized by a solid state reaction from a stoichiometric mixture of Er₂O₃ (99.9%) and SnO₂ (99.996%). The powder was ground and heated for 6–8 h four times from 1400 to 1450°C in air, cooled down to room temperature, and reground after each calcination.

An important issue regarding the measurements at very low temperature concerns the thermalization of the powder sample. For magnetization measurements, a few milligrams of Er₂Sn₂O₇ were mixed with apiezon N grease in a copper pouch, to improve the thermal contact and reduce the thermalization time. For neutron scattering experiments, a dedicated vanadium cell was used in the dilution fridge. The cell was filled with He gas up to 40 bars. During the experiments, it became obvious that a non negligible heating was induced by the sample's activation in the neutron beam. This effect was all the more important that the incident flux was large. Special care was then taken to minimize this effect for a better temperature control. For INS measurements, the neutron flux was reduced with a lead attenuator. For diffraction measurements, short counting times (of about 30 min) were programmed, alternating with deactivation (hence cooling) periods of 1 h. This thermalization issue probably explains why the transition had not been reported in previous neutron scattering measurements.

Zero field cooled - field cooled (ZFC-FC) magnetization measurements show an antiferromagnetic transition at $T_N = 108 \pm 5$ mK (see inset of Figure 2). It manifests as a peak in the ZFC curve, while the FC magnetization sharply increases at the transition. This effect, although less pronounced, is similar to what is observed in Er₂Ti₂O₇ [10] and could be due to the polarization of uncompensated magnetic moments at domain boundaries. This magnetic transition is also evidenced by a peak at T_N in the real part of the ac susceptibility (see top of Figure 2). A frequency dependent signal comes on top of this peak, as a bump which moves towards high temperature when the frequency increases. This bump is the signature of slow dynamics (already reported at higher temperatures [4]), which is not affected by the transition. The peak in the imaginary part of the ac susceptibility follows the same thermal activated Arrhenius behavior above and below the Néel temperature, with an energy barrier of about 0.9 K (see bottom inset of Figure 2).

Neutron diffraction confirms the presence of antiferromagnetic ordering at very low temperature, as shown in

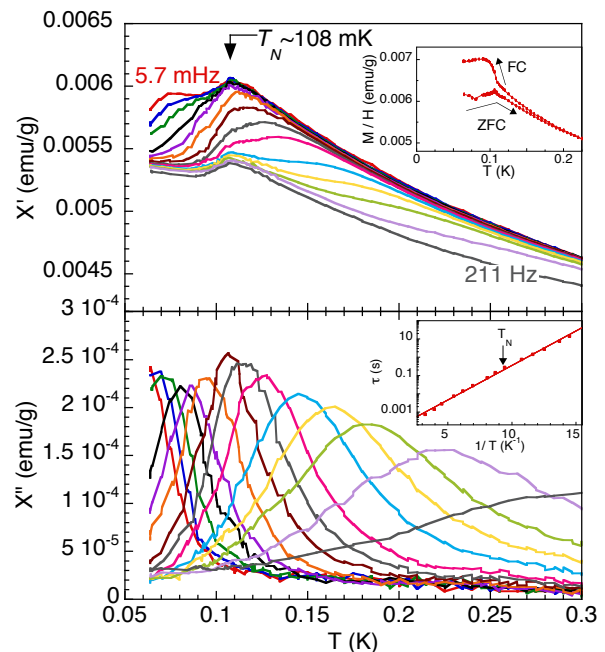


FIG. 2. (Color online) Ac susceptibility χ' (top) and χ'' (bottom) vs temperature T measured for several frequencies f between 5.7 mHz and 211 Hz, with $\mu_0 H_{ac} = 0.1$ mT. Top inset: Magnetization M/H vs T measured in a ZFC-FC procedure with $\mu_0 H = 1$ mT. Bottom inset: Relaxation time $\tau = 1/2\pi f$ vs $1/T$ extracted from the maxima of χ'' . The line is a fit with the Arrhenius law: $\tau = \tau_0 \exp(E/k_B T)$ with $\tau_0 \approx 6 \times 10^{-5}$ s and $E/k_B \approx 0.9$ K.

Figure 3. Intensity increases on existing crystalline Bragg peak positions, indicating a $\mathbf{k} = \mathbf{0}$ propagation vector. The main magnetic peaks appear at 1.07 and 1.22 Å⁻¹, corresponding to the $Q = (111)$ and (002) wavevectors, and emerge from the diffuse scattering signal characteristic of short-range Palmer-Chalker correlations [4, 8]. The latter has almost disappeared at the lowest temperature ($T = 68$ mK), indicating that most of the magnetic moment is ordered (see Figure 3(a)). Rietveld refinements show that, among the possible irreducible representations authorized by the $\mathbf{k} = \mathbf{0}$ propagation vector [6], neutron intensities can only be properly modeled by the Γ_7 representation, which corresponds to the Palmer-Chalker configuration. At the lowest temperature, the ordered moment is $3.1 \mu_B$, i.e. about 80 % of the total magnetic moment of the Er³⁺ ion (see Figure 3(b)). The remaining Er³⁺ moments are embedded in short-range only Palmer-Chalker correlations, as reflected by the persistence of a weak diffuse signal. This ordered moment value is consistent with what is expected in a conventional second order phase transition at the corresponding T/T_N ratio. The second order nature of the transition is further confirmed by the gradual increase of the ordered moment below T_N (see inset of Figure 3(b)).

We now focus on the excitation spectrum associated

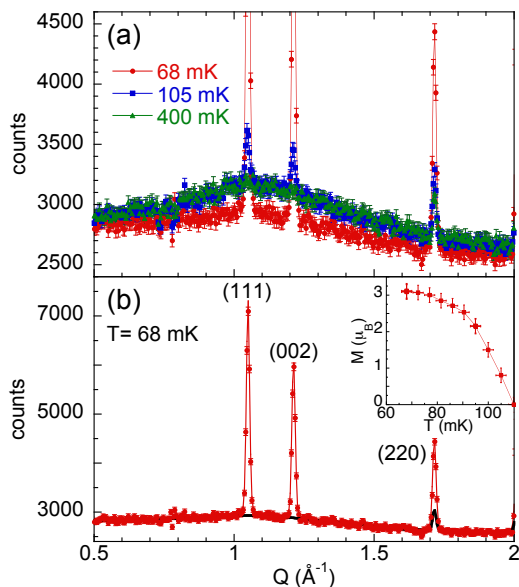


FIG. 3. (Color online) (a) Diffractograms at 68 mK (red), 105 mK (blue) and 400 mK (green). (b) Diffractogram at 68 mK. The black line is the fit corresponding to the nuclear contribution plus the diffuse Palmer-Chalker scattering. The red one shows the fit of the whole signal, including the magnetic long range Palmer-Chalker contribution. Inset: Temperature dependence of the ordered magnetic moment deduced from the refinements.

with this magnetic ordering. As previously reported, at temperatures as high as 10 K, the INS spectrum includes a strong quasielastic signal [8]. Its intensity is stronger around $Q_o = 1.1 \text{ \AA}^{-1}$, which corresponds to the position of the maximum intensity of the Palmer-Chalker diffuse scattering (see Figure 4(a)). On cooling, the intensity increases, while the width decreases, corresponding to a slowing down of the fluctuations, reaching a characteristic time of about 10^{-11} s close to T_N . This quasielastic signal persists down to temperatures below T_N (see Figure 4(b)). Nevertheless, because of self-heating in the neutron beam, the effective temperature actually reached by the sample at the lowest temperature of the dilution fridge ($T_{\min} = 70$ mK), is estimated to be 105 mK from the intensity of the magnetic Bragg peaks, thus just below T_N (corresponding to an ordered moment of $0.8 \mu_B$). Additional features, stemming from the Bragg peaks at $Q \approx 1$ and 1.2 \AA^{-1} , also arise in the ordered regime (see Figure 4(b)). In the cut shown in Figure 4(d), this additional signal manifests as a broad band in the $0.2 \leq \omega \leq 0.5$ meV range, superimposed on the quasielastic response.

To further analyze these results, we have refined the exchange parameters previously estimated from magnetization measurements [4]. To this end, we have used the well-documented procedure [12, 13], which consists in applying a magnetic field to drive the ground state towards

a field polarized state and analyze the spin excitations in terms of conventional spin waves. Owing to the polycrystalline nature of the $\text{Er}_2\text{Sn}_2\text{O}_7$ sample, the magnetic field is applied simultaneously in all crystallographic directions, leading to an average excitation spectrum. INS measurements were performed as a function of magnetic field at 1.5 K. Above about $\mu_o H = 1.5$ T, the response is no more quasielastic-like, and a dispersive spectrum is observed, with the opening of a gap (see Figure 5(a)). Its value is $\Delta = 0.26 \pm 0.04$ meV at $Q_o = 1.1 \text{ \AA}^{-1}$ for a field of $\mu_o H = 2$ T. Δ increases roughly linearly further increasing the field, as illustrated in Figure 5(c).

To determine the exchange parameters, we consider the following Hamiltonian:

$$\mathcal{H} = \mathcal{H}_{\text{CEF}} + \frac{1}{2} \sum_{\langle i,j \rangle} \mathbf{J}_i \tilde{\mathcal{J}} \mathbf{J}_j + g_J \mu_B \mathbf{H} \cdot \mathbf{J}_i$$

\mathbf{J} is the Er^{3+} magnetic moment, \mathcal{H}_{CEF} is the crystal electric field (CEF) Hamiltonian, \mathbf{H} denotes the magnetic field, g_J is the effective g factor, and $\tilde{\mathcal{J}}$ is the anisotropic exchange tensor, which incorporates the dipolar interaction truncated to its nearest neighbors. It is written in the $(\mathbf{a}_{ij}, \mathbf{b}_{ij}, \mathbf{c}_{ij})$ frame linked with Er^{3+} - $\text{Er}^{3+} \langle ij \rangle$ nearest neighbors bonds [14]:

$$\begin{aligned} \mathbf{J}_i \tilde{\mathcal{J}} \mathbf{J}_j = & \sum_{\mu, \nu=x,y,z} J_i^\mu D_{\text{nn}} (a_{ij}^\mu a_{ij}^\nu + b_{ij}^\mu b_{ij}^\nu - 2c_{ij}^\mu c_{ij}^\nu) J_j^\nu \\ & + \sum_{\mu, \nu=x,y,z} J_i^\mu (\mathcal{J}_a a_{ij}^\mu a_{ij}^\nu + \mathcal{J}_b b_{ij}^\mu b_{ij}^\nu + \mathcal{J}_c c_{ij}^\mu c_{ij}^\nu) J_j^\nu \\ & + \mathcal{J}_4 \sqrt{2} \mathbf{b}_{ij} \cdot (\mathbf{J}_i \times \mathbf{J}_j) \end{aligned}$$

where $D_{\text{nn}} = \frac{\mu_o}{4\pi} \frac{(g_J \mu_B)^2}{r_{\text{nn}}^3} = 0.022$ K is the pseudo-dipolar contribution (with r_{nn} the nearest neighbor distance in the pyrochlore lattice), \mathcal{J}_a , \mathcal{J}_b , \mathcal{J}_c are effective exchange parameters, and \mathcal{J}_4 corresponds to the antisymmetric Dzyaloshinski-Moriya interaction. This model takes into account the specific CEF scheme which strongly confines the spins within the local XY planes [4]. The powder average of the spin excitation spectrum $S(Q, \omega)_H$ is then calculated for a given field \mathbf{H} using the random phase approximation (RPA).

To compare with the polycrystalline experimental data shown in Figure 5(a), the average over all field directions has to be performed. As a first approximation, we consider that the powder spectrum can be described by averaging over the high symmetry directions of the system, $\langle 001 \rangle$, $\langle 110 \rangle$ and $\langle 111 \rangle$, taking into account their multiplicity. The weighted averaged spectrum then writes $\bar{S}(Q, \omega) = \frac{1}{13} (3S(Q, \omega)_{\mathbf{H} \parallel [001]} + 6S(Q, \omega)_{\mathbf{H} \parallel [110]} + 4S(Q, \omega)_{\mathbf{H} \parallel [111]})$. Assuming $\mathcal{J}_4 = 0$, since the Dzyaloshinski-Moriya is expected to be small compared to symmetric exchange, the best agreement is obtained with $\mathcal{J}_a = \mathcal{J}_b = 0.03 \pm 0.003$ K, $\mathcal{J}_c = 0.05 \pm 0.01$ K, thus consistent with the uncertainty range

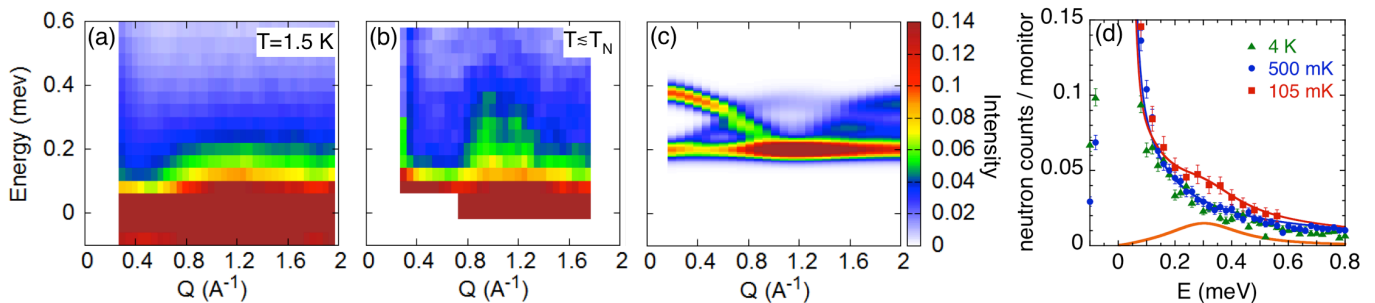


FIG. 4. (Color online) Inelastic neutron scattering in zero field: powder averaged spectrum $S(Q, \omega)$ measured (a) at 1.5 K, (b) below T_N , at about 105 mK. The neutron intensity is normalized to the monitor. Constant energy-scans were carried out to minimize self-heating effects. (c) Excitation spectrum in the Palmer-Chalker phase obtained from RPA calculations with the exchange parameters $\mathcal{J}_a = \mathcal{J}_b = 0.03$ K, $\mathcal{J}_c = 0.05$ K and $\mathcal{J}_d = 0$ at $T = 0$. (d) Energy cuts averaged for $1 \leq Q \leq 1.2 \text{ \AA}^{-1}$ at several temperatures: 4 K (green triangles), 500 mK (blue dots), 105 mK (red squares). The blue line is a fit involving a Gaussian profile, centered at zero energy to model the elastic response, and a quasielastic contribution $(1 + n(\omega)) \times A\omega\Gamma/(\omega^2 + \Gamma^2)$. $1 + n(\omega)$ is the detailed balance factor, $A = 0.2$ and $\Gamma = 0.046$ meV. The red line contains an additional inelastic contribution, shown separately by the orange line, and described by a Lorentzian profile $(1 + n(\omega)) \times B\gamma(1/[(\omega - \omega_o)^2 + \gamma^2] - 1/[(\omega + \omega_o)^2 + \gamma^2])$ with $B = 0.016$, $\omega_o = 0.3$ meV and $\gamma = 0.016$ meV.

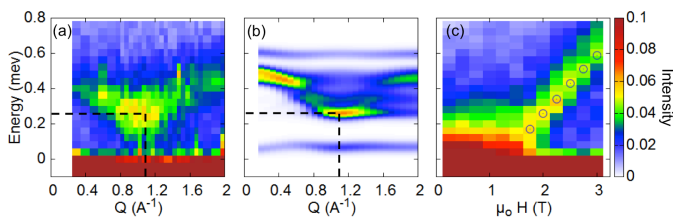


FIG. 5. (Color online) Inelastic neutron scattering in the field polarized phase. (a) Powder average spectrum $S(Q, \omega)$ measured at $T = 1.5$ K with $\mu_0 H = 2$ T. (b) Calculated powder average spectrum $S(Q, \omega)$ at 2 T and $T = 0$ with $\mathcal{J}_a = \mathcal{J}_b = 0.03$ K, $\mathcal{J}_c = 0.05$ K and $\mathcal{J}_d = 0$. (c) Powder average spectrum at $Q_o = 1.1 \text{ \AA}^{-1}$ and at $T = 1.5$ K as a function of field H . The empty blue circles are the values of the gap obtained from the calculations with the above parameters. The neutron intensity is normalized to the monitor.

given in Ref. 4. Calculations reproduce the strong intensity close to Q_o and the presence of a gap of about 0.25 meV (see Figure 5(b)). They also account for the field dependence of the gap at Q_o above 1.5 T, as shown in Figure 5(c) by the blue open circles. RPA calculations performed with these exchange parameters at $T = 0$ in zero field, predict a gapped flat mode at 0.2 meV, together with excitations dispersing up to 0.4 meV (see Figure 4(c)). While the value of the gap is consistent with the measured inelastic contribution, the predicted dispersion is hardly distinguishable in the data of Figure 4(b).

It is instructive to compare the $\text{Er}_2\text{Sn}_2\text{O}_7$ behavior with results obtained on $\text{Gd}_2\text{Sn}_2\text{O}_7$. The latter, in which the Gd^{3+} magnetic moment is almost isotropic, is known as the archetype of the dipolar *Heisenberg* pyrochlore antiferromagnet. In spite of very different anisotropies in both compounds, calculations predict identical behav-

iors, for thermodynamic and dynamical properties: the transition towards the Palmer-Chalker phase is expected to be first order [7, 16], while a spin wave spectrum, similar to Figure 4(c), should develop at low temperature, consisting in dispersive branches on top of a gapped flat mode [11, 17, 18]. $\text{Gd}_2\text{Sn}_2\text{O}_7$ indeed follows these predictions [19, 20], and the opening of the gap occurs well above T_N [21]. In $\text{Er}_2\text{Sn}_2\text{O}_7$, the scenario appears more complex: the temperature dependence of the ordered magnetic moment points out a second order transition. The lack of clear dispersion in the experimental INS spectrum might be attributed, in a classical picture, to the proximity of T_N . However, the strong XY character of the system, which can lead to unconventional excitations as lines of vortices [22], insufficiently captured by the RPA, might also explain the observed peculiar Q dependence of the spectrum.

The strong ratio between dipolar and exchange interactions in $\text{Er}_2\text{Sn}_2\text{O}_7$, which is about 0.5 – 0.7 (against 0.15 in $\text{Gd}_2\text{Sn}_2\text{O}_7$ [17]) also appears crucial. Preliminary calculations with $\text{Er}_2\text{Sn}_2\text{O}_7$ parameters at $T = 0$ and $Q = (1, 1, 1)$ show that accounting for the long range part of the dipolar interaction beyond the truncation considered above and in Ref. 4 and 7, slightly reduces the gap value, but does not affect the ground state. It was however established in Heisenberg systems that, at finite temperature, long range dipolar interactions tend to weaken the Palmer-Chalker state stability, due to the proximity of an unconventional state with a $\mathbf{k} = (1/2, 1/2, 1/2)$ propagation vector [23, 24] (proposed to be the magnetic state stabilized in $\text{Gd}_2\text{Ti}_2\text{O}_7$ [25]). The proximity of $\text{Er}_2\text{Sn}_2\text{O}_7$ with such a state, in addition to the proximity with the ψ_2 state evoked above, might reinforce the fluctuations in the Palmer-Chalker state at finite temperature and explain the structure of the spectrum close

to the transition. Note that the very low temperature considered here could suggest a role of quantum fluctuations, but they have been shown not to destabilize much the Palmer-Chalker state [7, 11].

Finally, in addition to the fast fluctuations observed in inelastic neutron scattering, slow dynamics appears above T_N and coexists with the magnetic ordering. Its characteristic energy barrier of 0.9 K ($= 0.078$ meV) is smaller than the gap of the Palmer-Chalker state. It might be associated with the spins at the boundary between the six existing domains, as previously reported in kagome and pyrochlore systems [26, 27].

We have shown that the pyrochlore $\text{Er}_2\text{Sn}_2\text{O}_7$ orders in the Palmer-Chalker state at about 100 mK. As confirmed by the analysis of the exchange couplings, it is the realization of the dipolar XY pyrochlore antiferromagnet. The absence of a first order transition along with multi-scale dynamics are signatures of an unconventional magnetic state. Further calculations, accounting for the XY character and for the long range dipolar interactions at finite temperature are needed to understand the role of fluctuations and enlighten the existence of exotic excitations. The proximity of $\text{Er}_2\text{Sn}_2\text{O}_7$ with competing phases might also enhance fluctuations, as recently proposed in the context of another pyrochlore compound $\text{Yb}_2\text{Ti}_2\text{O}_7$ [28, 29]. In that perspective, our study points out the importance of multiphase competitions in the novel magnetic states emerging in frustrated systems.

* sylvain.petit@cea.fr

† elsalhotel@neel.cnrs.fr

- [1] *Introduction to Frustrated Magnetism*, edited by C. Lacroix, P. Mendels, and F. Mila (Springer-Verlag, Berlin, 2011).
- [2] J. Villain, R. Bidaux, J.-P. Carton, and R. Conte, *J. Phys.* **41**, 1263 (1980).
- [3] E. F. Shender, *Zh. Eksp. Teor. Fiz.* **83**, 326 (1982) [*Sov. Phys. JETP* **56**, 178 (1982)].
- [4] S. Guitteny, S. Petit, E. Lhotel, J. Robert, P. Bonville, A. Forget, and I. Mirebeau, *Phys. Rev. B* **88**, 134408 (2013).
- [5] S. E. Palmer, and J. T. Chalker, *Phys. Rev. B* **62**, 488 (2000).
- [6] A. Poole, A. S. Wills, and E. Lelièvre-Berna, *J. Phys.: Condens. Matter* **19**, 452201 (2007).
- [7] H. Yan, O. Benton, L. D. C. Jaubert, and N. Shannon, arXiv:1311.3501; *Phys. Rev. B* **95**, 094422 (2017).
- [8] P. M. Sarte, H. J. Silverstein, B. T. K. Van Wyk, J. S. Gardner, Y. Qiu, H. D. Zhou, and C. R. Wiebe, *J. Phys.: Condens. Matter* **21**, 382201 (2011).
- [9] C. Paulsen, in *Introduction to Physical Techniques in Molecular Magnetism: Structural and Macroscopic Techniques - Yesa 1999*, edited by F. Palacio, E. Ressouche, and J. Schweizer (Servicio de Publicaciones de la Universidad de Zaragoza, Zaragoza, 2001), p. 1.
- [10] O. A. Petrenko, M. R. Lees, and G. Balakrishnan, *J. Phys.: Condens. Matter* **23**, 164218 (2011).
- [11] A. G. Del Maestro, and M. J. P. Gingras, *J. Phys.: Condens. Matter* **16**, 3339 (2004).
- [12] L. Savary, K. A. Ross, B. D. Gaulin, J. P. C. Ruff, and L. Balents, *Phys. Rev. Lett.* **109**, 167201 (2012).
- [13] K. A. Ross, L. Savary, B. D. Gaulin, L. Balents, *Phys. Rev. X* **1**, 021002 (2011).
- [14] B. Z. Malkin, T. T. A. Lummen, P. H. M. van Loosdrecht, G. Dhahenne, and A. R. Zakirov, *J. Phys.: Condens. Matter* **22**, 276003 (2010).
- [15] A. S. Wills, M. E. Zhitomirsky, B. Canals, J. P. Sanchez, P. Bonville, P. Dalmas de Réotier, and A. Yaouanc, *J. Phys.: Condens. Matter* **18**, L37 (2006).
- [16] O. Cepas, A. P. Young, and B. S. Shastry, *Phys. Rev. B* **72**, 184408 (2005).
- [17] A. Del Maestro, and M. J. P. Gingras, *Phys. Rev. B* **76**, 064418 (2007).
- [18] S. S. Sosin, L. A. Prozorova, P. Bonville, and M. E. Zhitomirsky, *Phys. Rev. B* **79**, 014419 (2009).
- [19] P. Bonville, J. A. Hodges, M. Ocio, J. P. Sanchez, P. Vulliet, S. Sosin, and D. Braithwaite, *J. Phys.: Condens. Matter* **15**, 7777 (2003).
- [20] J. R. Stewart, J. S. Gardner, Y. Qiu, and G. Ehlers, *Phys. Rev. B* **78**, 132410 (2008).
- [21] S. S. Sosin, L. A. Prozorova, A. I. Smirnov, P. Bonville, G. Jasmin-LeBras, and O.A. Petrenko, *Phys. Rev. B* **77**, 104424 (2008).
- [22] R. Savit, *Phys. Rev. B* **17**, 1340 (1978).
- [23] M. Enjalran, and M. J. P. Gingras, arXiv:0307152.
- [24] O. Cepas, and B. S. Shastry, *Phys. Rev. B* **69**, 184402 (2004).
- [25] J. D. M. Champion, A. S. Wills, T. Fennell, S. T. Bramwell, J. S. Gardner, and M. A. Green, *Phys. Rev. B* **64**, 140407(R) (2001).
- [26] E. Lhotel, V. Simonet, J. Ortloff, B. Canals, C. Paulsen, E. Suard, T. Hansen, D. J. Price, P. T. Wood, A. K. Powell, and R. Ballou, *Phys. Rev. Lett.* **107**, 257205 (2011).
- [27] S. Tardif, S. Takeshita, H. Ohsumi, J.I. Yamaura, D. Okuyama, Z. Hiroi, M. Takata, and T.H. Arima, *Phys. Rev. Lett.* **114**, 147205 (2015).
- [28] J. Robert, E. Lhotel, G. Remenyi, S. Sahling, I. Mirebeau, C. Decorse, B. Canals, and S. Petit, *Phys. Rev. B* **92**, 064425 (2015).
- [29] L. D. C. Jaubert, O. Benton, J. G. Rau, J. Oitmaa, R. R. P. Singh, N. Shannon, and M. J. P. Gingras, *Phys. Rev. Lett.* **115**, 267208 (2015).